Drought-induced reduction in temperature dependence of respiration decelerates net carbon loss with autumn warming in northern ecosystems

Dan Liu[1], Shilong Piao[1,2,3,4], Tao Wang[1,2], Xuhui Wang[5], Xiaoyi Wang[1], Jinzhi Ding[1], Philippe Ciais[5], Josep Peñuelas[6,7], and Ivan Janssens[8]

[1]Key Laboratory of Alpine Ecology and Biodiversity, Institute of Tibetan Plateau Research, Chinese Academy of Sciences, Beijing, China,

[2]Center for Excellence in Tibetan Earth Science, Chinese Academy of Sciences, Beijing, China,

[3]Sino-French Institute for Earth System Science, College of Urban and Environmental Sciences, Peking University, Beijing, China,

[4]University of Chinese Academy of Science, Beijing, China,

[5]Laboratoire des Sciences du Climat et de l'Environnement CEA CNRS UVSQ, Gif-sur-Yvette, France,

[6]CREAF, Cerdanyola del Valles, Spain,

[7]CSIC, Global Ecology Unit CREAF-CEAB-CSIC-UAB,Cerdanyola del Valles, Spain,

8Department of Biology, University of Antwerp, Wilrijk, Belgium

Boreal and arctic ecosystems are highly sensitive to climate change, with the northern high-latitude region warming faster than the global average (IPCC, 2013). Most previous studies on the response of the terrestrial carbon cycle to warming have focused on the net carbon uptake period (Lafleur et al., 2007; Richardson et al., 2009; Piao et al., 2017), while much less attention was paid on the dormant season, during which net carbon release occurs. Understanding how net carbon exchanges from the dormant season respond to warming is, however, equally crucial for forecasting ecosystem–carbon cycle feedbacks. Here, we present findings on the long-term effects of climate change on high-latitude ecosystem carbon cycle during the dormant season from the atmospheric CO_2 concentration record (Point Barrow, Alaska). We show that over the full study period (1974−2014), warming has significantly boosted autumn net carbon loss and advanced the CO_2 sink-source transition date, in line with previous analyses (Piao et al., 2008). However, in the second half of the study period, the atmospheric CO_2 record indicates no correlation between autumn net carbon loss and warming, which is further supported by analyses of net biome production from two different atmospheric inversion systems. Based on multiple sources of satellite-based productivity data, a suite of state-of-the-art ecosystem models and an atmospheric transport model, we further suggest that this deceleration of carbon losses with warming can be attributed to the loss of temperature dependency in respiration due to the soil moisture reduction, instead of changing temperature-productivity relationship, and changes in atmospheric transport, fossil fuel emissions and air-sea CO_2 exchanges. Our findings suggest that a warming climate does not necessarily result in a higher autumn CO_2 release, which offsets recently reported warming-induced loss of net carbon uptake during spring and summer seasons (Piao et al., 2017; Peñuelas et al., 2017) and therefore provide a negative feedback to climatic warming.

The northern land region that includes the tundra and boreal forests is acknowledged to be an important component of the global carbon cycle, accounting for a considerable land-based sink for atmospheric CO_2 (McGuire et al., 2009; Pan et al., 2011). There is a wide recognition that climate change is having and will continue to have fundamental impacts on northern ecosystem carbon cycling and in turn on variations in atmospheric CO_2 (Beer et al., 2010; Keenan et al., 2014; McGuire et al., 2009; Heimann and Reichstein, 2008; Cox et al., 2000; Fiedlingstein et al., 2001; McGuire et al., 2009; Ahlström et al., 2012). Although studies of ecosystem responses to warming have mainly focused on spring and summer (Guerlet et al., 2013; Keenan et al., 2014; Piao et al., 2017), climate-carbon cycle interactions during the dormant season could be as crucial in modulating future climate change, due to the fact that a large portion of ecosystem carbon is stored in the soil (Wang et al., 2011; Commane et al., 2017), and a small fractional change in soil respiration with warming might significantly affect net ecosystem production and atmospheric CO_2. However, we still lack the satisfactory assessment how the overall CO_2 exchange responds to climate change during the dormant season.

Multiple lines of evidence that have recently emerged indicate that the response of carbon cycling to recent climate change since the late 1990s are different from the previous few decades (Piao et al., 2014; Piao et al., 2017; Peñuelas et al., 2017; Ballantyne et al., 2017). It has long been assumed that warming advances spring phenology and increases ecosystem carbon uptake (Keeling et al., 1996; Richardson et al., 2009). Although this was valid up to the 1990s, it no longer holds because of the weakening temperature control of spring net primary productivity (Piao et al., 2017). Furthermore, atmospheric CO_2 concentrations suggest that warm spring and summer-induced increases in annual CO_2 amplitude (the difference between the annual maximum and minimum concentrations within the same year), that could reflect the strength of net carbon uptake during

spring and summer disappeared in the last 17 years (Peñuelas et al., 2017). These multiple observational signals consistently reveal a shift in the warming effect on net carbon uptake from positive to neutral or even negative in spring and summer. However, it remains unclear how the effects of warming on net carbon release during the dormant season change with time. There is growing consensus that ecosystem productivity shows strong acclimation to warming (Oechel et al., 2000; Smith and Dukes, 2013), while respiratory flux to the atmosphere from ecosystem is anticipated to increase with warming. We therefore formulate the hypothesis that warming can accelerate net carbon loss during the dormant season and exacerbate negative warming impact on annual carbon sequestration.

We studied this hypothesis by analyzing the relationship between indicators of net carbon release inferred from atmospheric CO_2 and temperature during the dormant season, and its temporal change over the period 1974−2014. We calculated partial correlation coefficient between net carbon release during the dormant season (defined as the change of CO_2 concentration from September to November for autumn and from December to next April for winter at Point Barrow, Alaska) and temperature in boreal and arctic ecosystems north of 50°N (through removing statistical influence of precipitation and cloudiness variations, as detailed in Methods). There is a tight relationship between autumn net carbon release (ACR) and temperature on the inter-annual timescale over the period 1974−2014 ($R_{ACR\text{-}T}$ = -0.39, $P < 0.05$) (Figure S1), confirming that warming-induced increase in autumn respiration dominated over autumn photosynthetic gains (Piao et al., 2008; Miller, 2008). Unexpectedly, $R_{ACR\text{-}T}$ changed from -0.62 ($P < 0.01$) during 1974−1996 to -0.05 ($P = 0.85$) during 1997−2014, which runs counter to our proposed hypothesis that the negative temperature impact on annual carbon sequestration would recently become much

more pronounced. The observed diminished correlation between mean autumn temperature and ACR implies smaller land carbon release and reduced atmospheric CO_2 growth between September and November during warmer years. The sensitivity of ACR to autumn temperature ($\gamma_{ACR\text{-}T}$) shifts from -1.09 ppm K^{-1} during the earlier period to -0.11 ppm K^{-1} during later period (Figure S2), with change in magnitude of 0.98 ppm K^{-1}, indicating a change in sensitivity of about 2.09 gigatonnes of carbon per year per K when calculating based on a conversion factor of 2.14 GtC ppm^{-1} (IPCC, 2013). This diminished negative temperature effect on autumn carbon cycle is also detected in the upward zero-crossing date of CO_2 (defined as the day when detrended seasonal CO_2 crosses the zero line from the negative to positive value). In the earlier period warmer years implied earlier crossing dates (R = -0.66, P < 0.01), while in the later period no correlation remained (R = -0.02, P = 0.95) (Figure S3). In contrast to autumn, in winter no temperature response of ACR was detected, neither in the earlier period (R = 0.11, P = 0.63), nor in the later period (R = -0.04, P = 0.89) (Figure 1c).

To test the robustness of the observed decelerated loss of warming impact on autumn ACR, we performed the following additional analyses: (1) we defined autumn as the period from September 1st to the date when detrended seasonal CO_2 crosses the zero line from the negative to positive value (Figure S4), (2) we used another climate dataset (WFDEI, see Methods, Figure S5) and (3) we used CO_2 concentration records from weekly *in situ* measurements and flask samples (see Methods, Figure S6). All of these analyses confirmed that autumn warming no longer accelerates autumn net carbon release in the latest period. In a consistent manner, we also analyzed the temporal change in temperature dependence of net biome production (NBP) from two different atmospheric inversion systems. Consistent with the atmospheric CO_2 analyses, NBP from the Jena CarboScope inversion system also indicated a non-significant temperature impact on autumn NBP

over boreal and arctic ecosystems north of 50°N during 1997−2011 (R = -0.44 ± 0.13), in contrast to the significant temperature effect found during 1982−1996 (R = -0.74 ± 0.05) (Figure 2a). Similar results were also found if NBP from MACC inversion system was considered (1982−1996: R = -0.65 ± 0.08; 1997−2011: R = -0.16 ± 0.15, Figure S7). Besides land ecosystems, atmospheric CO_2 variation also harbors signals from changes in atmospheric transport, air-sea CO_2 exchanges and fossil fuel emissions. We therefore assessed their potential contributions to the change in $R_{ACR\text{-}T}$ using atmospheric transport simulations based upon atmospheric transport model from the Laboratoire de Météorologie Dynamique (LMDz) (Hourdin et al., 2006) (see Methods), and found that their decadal changes would not contribute to the observed diminished temperature control on ACR (Figure S8).

Which terrestrial carbon cycle processes caused the diminished negative temperature control on the autumn carbon cycle in the north? This diminished effect could be only explained by an enhanced temperature reliance of carbon uptake through vegetation photosynthesis and/or a reduced temperature dependence of carbon loss through respiration. Analysis of satellite-based vegetation index (GIMMS NDVI) (Tucker et al., 2005) as a proxy for vegetation production showed that autumn NDVI is marginally significantly correlated with temperature in the earlier period (R = 0.50 ± 0.15), but became decoupled from temperature in the later period (R = -0.37 ± 0.14) (Figure S9). This weakened temperature dependence of vegetation production was, nonetheless, also evident when considering satellite-based estimates of net primary productivity (NPP) (Smith et al., 2016, Figure 2b), or satellite-independent estimates of gross primary productivity (GPP) up-scaled from eddy flux towers (Jung et al., 2009)(Figure S10), thereby ruling out its possibility in explaining the diminished temperature effect on ACR. For example, $R_{NPP\text{-}T}$

and $R_{GPP\text{-}T}$ decreased from 0.82 ± 0.06 and 0.88 ± 0.04 in the earlier period to 0.41 ± 0.23 and 0.43 ± 0.14 in the later period, respectively.

The heterotrophic respiration (HR), computed as the difference between NBP from Jena CarboScope (or MACC) dataset and satellite-derived NPP, has significant partial correlations with autumn temperature in the earlier period (Jena: $R_{HR\text{-}T}$ = 0.90 ± 0.03; MACC: $R_{HR\text{-}T}$ = 0.79 ± 0.06) but not in the later period (Jena: $R_{HR\text{-}T}$ = 0.48 ± 0.14; MACC: $R_{HR\text{-}T}$ = 0.28 ± 0.15) (Figure 2c, Figure S7b). Furthermore, we also analyzed simulated HR from eight models participating in the historical climate carbon cycle model intercomparison project (TRENDY, see Methods), and found that the strong HR-temperature correlation in the earlier period also became weak and non-significant during the later period across almost all of the models (Figure S11 and S12). Therefore, we conclude that the diminished negative temperature effect on autumn carbon cycle during the latest period is most likely due to diminished temperature dependence of respiratory losses. To diagnose the potential mechanism responsible for the decrease in $R_{HR\text{-}T}$, we studied decadal changes in simulated soil moisture content from TRENDY models, and found a widespread reduction in soil moisture particularly over North America and Siberia, which was spatially coherent with the decline in $R_{HR\text{-}T}$, suggesting the plausibility of a potential soil water effect (Figure S13).

We provide the evidence that autumnal warming no longer accelerates net carbon losses and advance the end of the carbon uptake period in boreal and arctic ecosystem as previously suggested (Piao et al., 2008; Ueyama et al., 2014), primarily through reducing positive decomposition responses to warming most likely due to a soil moisture shortage. The autumnal finding reveals the similar temperature-dependent shift in carbon cycle over the last 3 decades that is also found to occur in the main growing season (Peñuelas et al., 2017; Piao et al., 2017), suggesting a changing

paradigm for temperature control over ecosystem carbon cycling. However, the outcomes of these shifts on net CO_2 exchanges are not consistent in the direction of their effect on atmospheric pCO2 and would thus partly compensate for each other. The autumnal respiratory acclimation has an ameliorating impact on net CO_2 losses with rising temperatures, which could offset the negative warming impact on net CO_2 uptake during the active growing season (Peñuelas et al., 2017; Piao et al., 2017). It is therefore premature to conclude that the impact of temperature on annual carbon cycle has fundamentally shifted towards the negative state, and highlights the importance of incorporating how net carbon losses change with temperature during the dormant period in fully understanding temperature impacts on net carbon uptake. Additional studies are still needed to quantify whether these two opposing effects on carbon cycle will effectively neutralize each other, particularly for arctic and boreal ecosystems where the majority of permafrost soil carbon is stored and increasing old soil carbon will be respired to the atmosphere as a result of warming-induced permafrost thaw (Schuur et al., 2015; Pries et al., 2016; Koven et al., 2011).

Figure 1. Temperature control on net carbon release during the dormant season. Here we define the dormant season as the period from September to next April (**a**), which consists of autumn (September to November, **b**) and winter (December to next April, **c**). The lines are time series of the detrended anomaly of net carbon release (green) and mean temperature across land ecosystems north of 50°N (red).

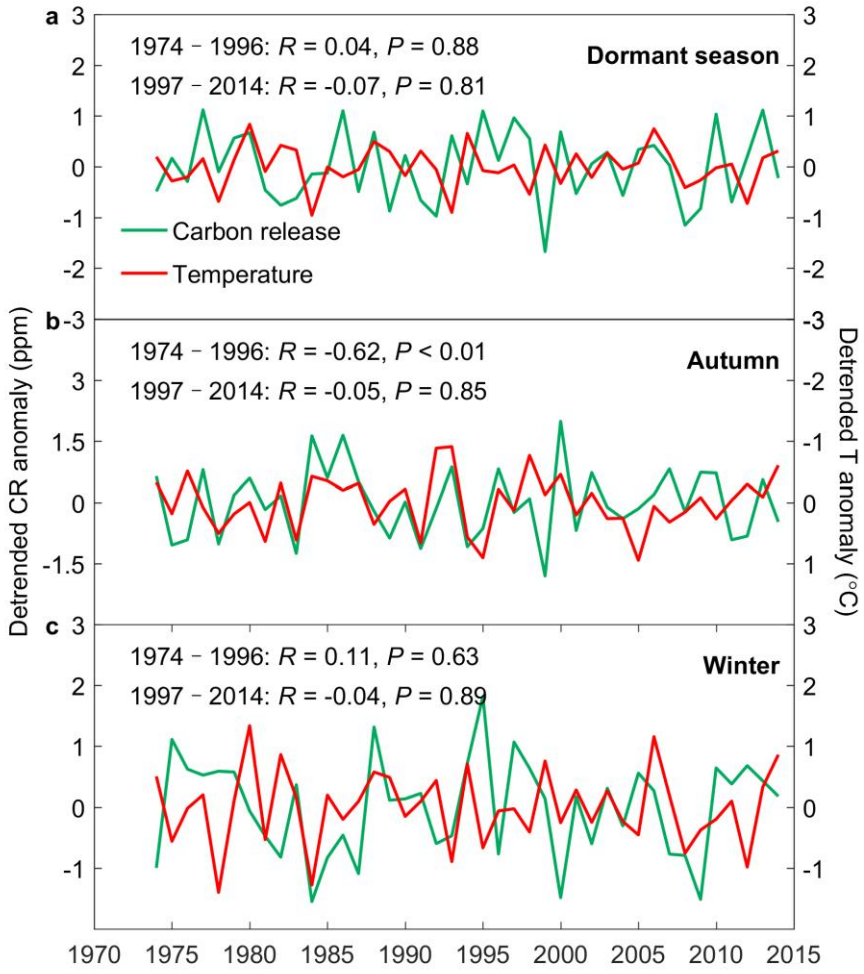

Figure 2. The relationship between ecosystem carbon fluxes and temperature in autumn. (**a-c**), the frequency distribution of the partial correlation coefficient of net biome production (NBP), net primary productivity (NPP), and heterotrophic respiration (HR) with average temperature during September to November across land ecosystem north of 50°N, whilst controlling for precipitation and cloudiness during the earlier period (1982−1996, blue bar) and later period (1997−2011, red bar), respectively. For each period, we randomly selected 12 years to generate the frequency distribution of partial correlation coefficient. The shade illustrates the significance level at $P < 0.05$ (magenta) and $P < 0.10$ (green), respectively. (**d-f**), the spatial distribution of the changes in the partial correlation coefficient of NBP, NPP and HR with temperature for the two periods, respectively. Here NBP is estimated from Jena CarboScope inversion system, the NPP is estimated based on GIMMS NDVI, and HR was calculated as the difference between NBP and NPP.

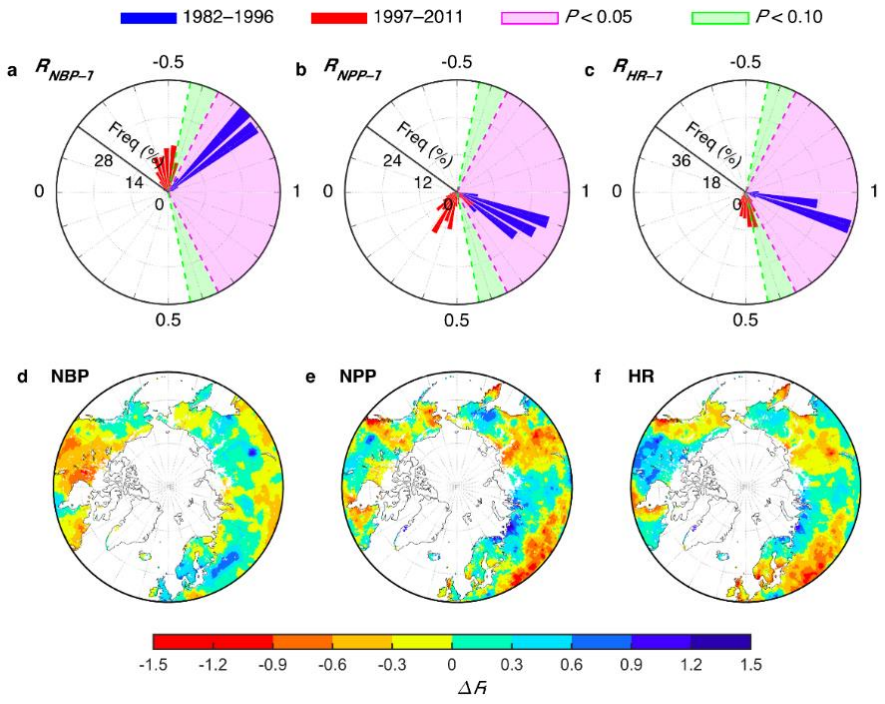

Figure 3. Schematic of the effect of warming on seasonal CO_2 uptake and release. In spring, warming advances the source-to-sink transition date and increases CO_2 uptake that decreases atmosphere CO_2 (Keeling et al., 1996), but which disappeared in the later period (1996−2012) (Piao et al., 2017). In summer, the effect of warming on net CO_2 uptake became significantly negative in the later period that increases atmosphere CO_2 (Peñuelas et al., 2017). On the contrary, the widely recognized autumn warming-induced advancement in sink-to-source transition date and acceleration in net CO_2 release (Piao et al., 2008) became diminished in the later period, which could decrease build-up of atmospheric CO_2. In contrast, the temperature effect on winter net CO_2 release is not significant during both periods.

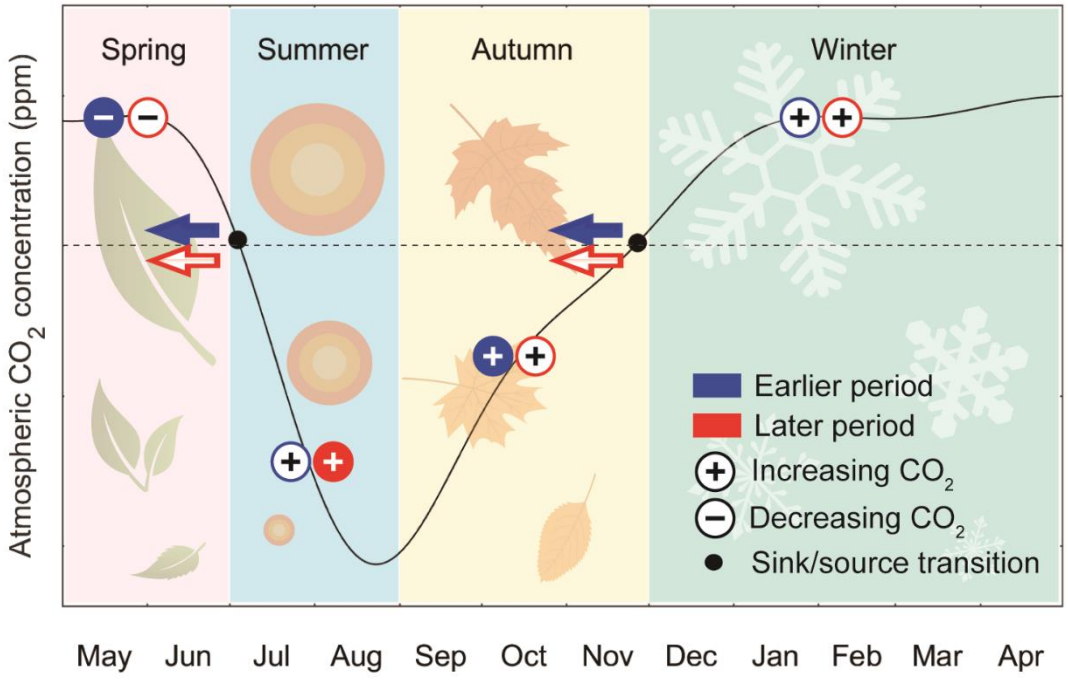

Materials and Methods

Atmospheric CO_2 concentration

The CO_2 concentration records from Point Barrow (71°N, Alaska) cover the period from 1974 to 2014, and are derived from the National Oceanic and Atmospheric Administration (NOAA) Earth System Research Laboratory (Thoning et al., 2014). The CO_2 concentration time series consist of three types of signals: the long-term trend, the short-term variations, and the seasonal cycle. We performed the following procedure to obtain detrended seasonal cycle of CO_2 concentration. First, we fitted the daily CO_2 records using a function consisting of four harmonics and a quadratic polynomial to separate the seasonal cycle from the long-term increasing trend (Thoning et al, 1989) and obtain the residuals from this function fit. Second, we used a 1.5 month (or 1 month, see Figure S6) full-width half-maximum value (FWHM) averaging filter to remove the short-term variations from the residuals and get a smoothed curve by adding the filtered residuals to the fitted function in the first step. We also applied a 390-day FWHM averaging filter to derived residuals from the first step and added the filtered residuals to the fitted long-term trend from quadratic polynomial to obtain a de-seasonalized long-term trend. Finally, we calculated the difference between the smoothed curve and the de-seasonalized long-term trend as the detrended seasonal CO_2 concentration. As outlier records have strong influence on the fitting process, we repeatedly fitted the CO_2 time series as described in the first step and discarded records lying outside five times of standard deviation of the residuals until no outliers were found (Harris et al, 2000).

We define the dormant season as the period from September to next April and calculated the changes in detrended CO_2 concentration during this period (CO_2 concentration in the last week of April in next year minus that in the first week of September) as the dormant season net carbon

release (CR). We also separate the dormant season into autumn (September to November) and winter (December to next April) and calculated autumn carbon release (ACR) and winter carbon release (WCR) as the changes of CO_2 concentration in autumn and winter, respectively. In addition, the mean date when detrended seasonal CO_2 crosses zero line from the negative to positive value is around the 317th day of the year (DOY) during the period from 1974 to 2014. To test the robustness of the analysis, we also defined autumn as the period from the first day of September to DOY 317 and defined winter as the period from DOY 318 to the last day of April in next year and calculated ACR and WCR accordingly. Furthermore, we also calculate CR from the weekly atmospheric CO_2 concentration from the NOAA Earth System Research Laboratory at Barrow.

Climate dataset

We used the monthly climate dataset from the Climate Research Unit, University of East Anglia (CRU TS4.0 dataset) (Mitchell et al, 2005) in this study. This dataset covers the period from 1901 to 2015, with a spatial resolution of 0.5°×0.5°. We selected mean temperature, precipitation and cloud cover for the analysis. We also used another climate dataset, which applied the WATer and global Change (WATCH) Forcing Data to the ERA-Interim dataset (http://www.eu-watch.org/gfx_content/documents/README-WFDEI.pdf) for the analysis and obtained similar results (Figure S5).

Vegetation production datasets

We used the Normalized Difference Vegetation Index (NDVI) retrieved from the third-generation of the Advanced Very High Resolution Radiometer (AVHRR) developed by the Global Inventory Modeling and Mapping Studies (GIMMS) group (version 3g.v0, available at

https://ecocast.arc.nasa.gov/data/pub/gimms/3g.v0) as a proxy for vegetation activity (Tucker et al, 2005). The GIMMS NDVI dataset covers the period from 1982 to 2013, with a spatial resolution of 0.083°×0.083°. We also used two vegetation production data: the monthly GIMMS net primary production (NPP) dataset (Smith et al, 2016), and the gross primary productivity (GPP) up-scaled from eddy flux towers using multi-tree ensemble approach (Jung et al, 2009).

Atmospheric CO_2 inversion data

We gathered two atmosphere CO_2 inversion products to investigate the response of terrestrial carbon fluxes to warming. We used monthly net biome production (NBP) from the Jena CarboScope (http://www.bgc-jena.mpg.de/CarboScope/, version s81_v3.8) for the period from 1982 to 2011, with a spatial resolution of 3.75º latitude ×5º longitude. The monthly net biome production (NBP) from the Monitoring Atmospheric Composition and Climate (Chevallier et al, 2005) (MACC, version v14r2, http://copernicus-atmosphere.eu/) between 1979 and 2011 was also used for the analysis. We calculated the heterotrophic respiration as the difference between inversed NBP and satellite-based NPP.

Terrestrial ecosystem models

Simulation results of eight models from a historical climate carbon cycle model inter-comparison project (Trendy) were used in this study. These models are Community land Model Version 4.5 (CLM4.5), the Integrated Science Assessment Model (ISAM), the Joint UK Land Environment Simulator (JULES), Lund-Potsdam-Jena DGVM (LPJ), Lund-Postam-Jena General Ecosystem Simulator (LPJ-GUESS), the Land surface Processes and eXchanges (LPX), the Organizing Carbon and Hydrology In Dynamic Ecosystems (ORCHIDEE), and the Vegetation Integrative Simulator for Trace gases (VISIT). All the models used forcing data from CRUNCEP dataset, and

the simulation setup follow the standard protocol described in the inter-comparison project (http://dgvm.ceh.ac.uk/files/Trendy_protocol%20_Nov2011_0.pdf). Here we used the S2 simulations, which consider the effect of climate change and rising CO_2 concentration on ecosystem carbon fluxes.

Effects of atmospheric transport, air-sea CO_2 exchanges and fossil fuel emission on the change in autumn net CO_2 release

To investigate the effects of atmospheric transport, air-sea CO_2 exchanges and fossil fuel emission on the change in autumn net carbon release, we assessed the impact of year-to-year variations in atmospheric transport, air-sea CO_2 exchange and fossil fuel emission on the observed changes on autumn net carbon release between the early period (1979−1996) and the later period (1997−2012) using atmospheric transport simulations. We used LMDz4, a 3D atmospheric tracer transport model from the Laboratoire de Météorologie Dynamique (Hourdin et al., 2006), nudged with ECMWF winds. As boundary conditions for transport simulations, we use land carbon fluxes over 1979–2012 from the land surface model ORCHIDEE (Krinner et al., 2005) that is driven by observed atmospheric CO_2 concentration and historical climate forcing from the CRU-NCEPv4 climate variables at 6-h resolution (Viovy and Ciais, 2014). For air–sea CO_2 exchanges, we use simulations from a biogeochemical model PlankTOM5 combined with a global ocean general circulation model NEMO (NEMO-PlankTOM5) that is forced by inputs of ions and compounds from river, sediment and dust for the PlankTOM5 model, and daily wind and precipitation from the NCEP reanalysis for the NEMO model (Buitenhuis et al., 2010). For fossil fuel CO_2 emissions, the monthly global time series was derived from the Carbon Dioxide Information Analysis Center (CDIAC) website (http://cdiac.esd.ornl.gov) (Andres et al,2011).

To assess whether changes in atmospheric transport can influence the observed change in ACR, we perform the transport modeling experiment in which land and air–sea CO_2 exchanges are fixed at the year 1979 but the atmospheric transport allows to be varying according to ECMWF wind fields (refer to WCC hereafter). For air–sea CO_2 exchange, we conduct the modeling experiment where the atmospheric transport and land carbon fluxes are fixed at year 1979 but air–sea CO_2 exchanges vary according to simulations from NEMO-PlankTOM5 (WAC simulation). To assess the effect from fossil fuel emission, we conducted the modeling experiment where the land and air-sea CO_2 exchanges fixed at the year 1979, but transport the year-to-year varying fossil fuel emission (WCF simulation).

Analysis

We performed partial correlation analysis between net carbon release during the dormant season (autumn and winter) with temperature whilst statistically controlling for precipitation and cloud cover ($R_{CR\text{-}T}$, $R_{ACR\text{-}T}$, and $R_{WCR\text{-}T}$). The climate variables are averaged over the region north of 50°N, and we only considered the pixels where the annual NDVI greater than 0.1. The partial correlation analysis was performed for the earlier period (1974-1996) and later period (1997-2014) respectively. All variables are detrended before the partial correlation analysis. For a more robust analysis, we also performed the partial correlation analysis through randomly selecting 12 years from the time series among the corresponding period to generate a frequency distribution of the partial correlation coefficient. We also conducted a two-sample *t*-test to determine whether the partial correlation coefficient is statistically significant. To test if the shift of $R_{ACR\text{-}T}$ is influenced by atmospheric transport, we calculated ACR from the WCC simulation, which all factors except wind field are fixed to year 1979, to denote the effect from atmospheric transport. To test if the

316 shift of $R_{ACR\text{-}T}$ is influenced by the transport of air-sea CO_2 and fossil fuel emission, we calculated
317 the air-sea CO_2 and fossil fuel induced ACR by calculating the difference between the WAC (WCF)
318 and the WCC simulation. Then we conducted the partial correlation analysis on the WAC (WCF)
319 induced ACR. To investigate the driver of the shift of $R_{ACR\text{-}T}$, we also performed the same analysis
320 to the satellite-derived NDVI ($R_{NDVI\text{-}T}$), the satellite-based NPP ($R_{NPP\text{-}T}$), the flux-tower based GPP
321 ($R_{GPP\text{-}T}$), the inversed NBP ($R_{NBP\text{-}T}$) and the HR calculated from NBP and NPP ($R_{HR\text{-}T}$).

References

1. IPCC. Climate Change 2013: The Physical Science Basis: Summary for Policymakers. (eds Stocker, T. F. et al.) (Cambridge University Press, Cambridge, 2013).

2. Lafleur, P. M & Humphreys, E. R. Spring warming and carbon dioxide exchange over low Arctic tundra in central Canada. *Glob. Change Biol.* **14**, 740-756 (2007)

3. Richardson, A. D. *et al*. Influence of spring phenology on seasonal and annual carbon balance in two contrasting New England forests. *Tree Physiol.* **29**, 321-221 (2009)

4. Piao, S. L. *et al*. Weakening temperature control on the interannual variations of spring carbon uptake across northern lands. *Nat. Clim. Change* **7**, 359-363 (2017)

5. Piao, S. L. *et al*. Net carbon dioxide losses of northern ecosystems in response to autumn warming. *Nature* **451**, 49-52 (2008)

6. Peñuelas, J. *et al*. Shifting from a fertilization-dominated to a warming-dominated period. Nature Ecology and Evolution, in press

7. McGuire, A. D. *et al.* Sensitivity of the carbon cycle in the Arctic to climate change. *Ecol. Monogr.* **79 (4)**, 523-555 (2009)

8. Pan, Y. D. *et al.* A large and persistent carbon sink in the world's forests. *Science* **333 (6045)**, 988-993 (2011)

9. Beer, C. *et al.* Terrestrial gross carbon dioxide uptake: global distribution and covariation with climate. *Science* **329 (5993)**, 834-838 (2010)

10. Keenan, T. F. *et al.* Net carbon uptake has increased through warming-induced changes in temperate forest phenology. *Nat. Clim. Change* **4**, 598-604 (2014)

11. Heimann, M. & Reichstein, M. Terrestrial ecosystem carbon dynamics and climate feedback. *Nature* **451**,289-292 (2008)

12. Ahlström, A. *et al.* Robustness and uncertainty in terrestrial ecosystem carbon response to CMIP5 climate change projections. *Environ. Res. Lett.* **7 (4)**, 044008 (9pp) (2012)

13. Cox, P. M. *et al.* Acceleration of global warming due to carbon-cycle feedbacks in a coupled climate model, *Nature* **408**, 184-187

14. Friedlingstein, P. *et al.* Positive feedback between future climate change and the carbon cycle, *Geophys. Res. Lett.*, **28 (8)**, 1543-1546

15. Guerlet, S. *et al.* Reduced carbon uptake during the 2010 Northern Hemisphere summer from GOSAT. *Geophys. Res. Lett.*, **40 (10)**, 2378-2383 (2013)

16. Wang, T. *et al.* Controls on winter ecosystem respiration in temperate and boreal ecosystems. *Biogeosciences* **8**, 2009-2025 (2011)

17. Commane, R. *et al.* Carbon dioxide sources from Alaska driven by increasing early winter respiration from Arctic tundra. *Proc. Natl. Acad. Sci. USA* **114 (21)**, 5361-5366 (2017).

18. Piao, S. L. *et al.* Evidence for a weakening relationship between interannual temperature variability and northern vegetation acitivity. *Nat. Commun.* **5018** doi: 10.1038/ncomms6018 (2014)

19. Ballantyne, A. *et al.* Accelerating net terrestrial carbon uptake during the warming hiatus due to reduced respiration, *Nat. Clim. Change* **7**, 148-152 (2017)

20. Keeling, C. D., Chin, J. F. S. & Whorf, T. P. Increasing activity of northern vegetation inferred from atmospheric CO_2 measurements. *Nature* **382**, 146-149 (1996)

21. Oechel, W. C. *et al.* Acclimation of ecosystem CO_2 exchange in the Alaskan Arctic in response to decadal climate warming. *Nature* **406**, 978-981 (2000)

22. Smith, N. G. & Dukes, J. S. Plant respiration and photosynthesis in global-scale models: incorporating acclimation to temperature and CO_2. *Glob. Change Biol.* **19 (1)**, 45-63 (2013)

23. Miller J. B. Carbon cycle: sources, sinks and seasons. *Nature* **451**, 26-27 (2008)

24. Hourdin, F. *et al.* The LMDZ4 general circulation model: climate performance and sensitivity to parametrized physics with emphasis on tropical convection. *Clim. Dynam.* **27**, 787-813 (2006).

25. Tucker, C. J. *et al.* An extended AVHRR 8−km NDVI dataset compatible with MODIS and SPOT vegetation NDVI data. *Int. J. Remote Sens.* **26**, 4485-4498 (2005)

26. Smith, W. K. *et al*. Large divergence of satellite and Earth system model estimates of global terrestrial CO_2 fertilization. *Nat. Clim. Change* **6**, 306-310 (2016)

27. Jung, M., Reichstein, M. & Bondeau, A. Towards global empirical upscaling of FLUXNET eddy covariance observations: validation of a model tree ensemble approach using a biosphere model. *Biogeosciences* **6**, 2001-2013 (2009).

28. Ueyama, M., Iwata, H. & Harazono, Y. Autumn warming reduces the CO_2 sink of a black spruce forest in interior Alaska based on a nine-year eddy covariance measurement. *Glob. Change Biol.* **20**, 1161-1173 (2014)

29. Schuur, E.A.G. *et al.* Climate change and the permafrost carbon feedback. *Nature* **520**, 171-179 (2015).

30. Pries, C. E. H. *et al.* Old soil carbon losses increase with ecosystem respiration in experimentally thawed tundra. *Nat. Clim. Change* **6**, 214-218 (2016)

31. Koven C. D., Ringeval B, Friedlingstein P, *et al.* Permafrost carbon-climate feedbacks accelerate global warming. *Proc. Natl. Acad. Sci. USA* **108 (36)**, 14769-14774 (2011).

32. Thoning, K. W., Kitzis, D. R. & Crotwell, A. Atmospheric Carbon Dioxide Dry Air Mole Fractions from Quasi-Continuous Measurements at Barrow, Alaska (NOAA ESRL Global Monitoring Division, 2014); ftp://aftp.cmdl.noaa.gov/data/trace_gases/co2/in-situ/surface/brw/co2_brw_surface-insitu_1_ccgg_DailyData.txt

33. Thoning, K.W., Tans, P. P. & Komhyr,W. D. Atmospheric carbon dioxide at Mauna Loa observatory. 2. Analysis of the NOAA GMCC data, 1974-1985. *J. Geophys. Res.* **94**, 8549-8565 (1989).

34. Harris, J. M. *et al.* An interpretation of trace gas correlations during Barrow, Alaska, winter dark periods, 1986-1997. *J. Geophys. Res.* **105**, 17267-17278 (2000).

35. Mitchell, T. D. & Jones, P. D. An improved method of constructing a database of monthly climate observations and associated high-resolution grids. *Int. J. Climatol.* **25**, 693-712 (2005).

36. Chevallier, F. *et al.* Inferring CO_2 sources and sinks from satellite observations: Method and application to TOVS data. *J. Geophys. Res.* **110,** D24309 (2005)

37. Hourdin, F. *et al.* The LMDZ4 general circulation model: climate performance and sensitivity to parametrized physics with emphasis on tropical convection. *Clim. Dynam.* **27**, 787-813 (2006).

38. Krinner, G. *et al.* A dynamic global vegetation model for studies of the couped atmosphere-biosphere system. *Global Biogeochem. Cy.* **19 (1)**, DOI: 10.1029/2003GB002199. (2005)

39. Viovy, N. & Ciais, P. CRUNCEP data set for 1901-2012 Tech. Rep. V. 4 (Laboratoire des Sciences du Climat et de l'Environnement, 2014); https://www.earthsystemgrid.org/browse/viewActivity.html?activityId=ff9d6ffbf0b9-11e2-aa24-00c0f03d5b7c

40. Buitenhuis, E. T. *et al.* Biogeochemical fluxes through microzooplankton. *Global Biogeochem. Cy.* **24(4)**, DOI: 10.1029/2009GB003601 (2010)

41. Andres, R. J. *et al*. Monthly, global emissions of carbon dioxide from fossil fuel consumption. *Tellus B* **63**, 309-327 (2011)